Faraday Discussions

Accepted Manuscript

This manuscript will be presented and discussed at a forthcoming Faraday Discussion meeting. All delegates can contribute to the discussion which will be included in the final volume.

Register now to attend! Full details of all upcoming meetings: http://rsc.li/fd-upcoming-meetings

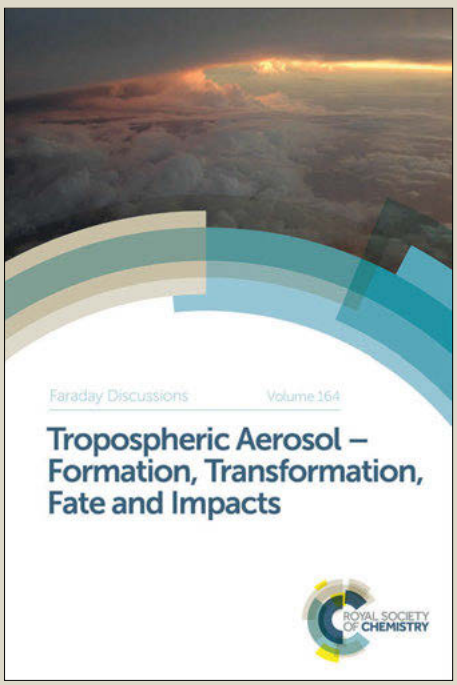

This is an *Accepted Manuscript*, which has been through the Royal Society of Chemistry peer review process and has been accepted for publication.

Accepted Manuscripts are published online shortly after acceptance, before technical editing, formatting and proof reading. Using this free service, authors can make their results available to the community, in citable form, before we publish the edited article. We will replace this *Accepted Manuscript* with the edited and formatted *Advance Article* as soon as it is available.

You can find more information about *Accepted Manuscripts* in the Information for Authors.

Please note that technical editing may introduce minor changes to the text and/or graphics, which may alter content. The journal's standard Terms & Conditions and the Ethical guidelines still apply. In no event shall the Royal Society of Chemistry be held responsible for any errors or omissions in this *Accepted Manuscript* or any consequences arising from the use of any information it contains.

ROYAL SOCIETY OF CHEMISTRY

www.rsc.org/faraday_d

Mechanically induced silyl ester cleavage under acidic conditions investigated by AFM-based single-molecule force spectroscopy in the force-ramp mode

Sebastian W. Schmidt,[abc] Michael F. Pill,[abc] Alfred Kersch,[a] Hauke Clausen-Schaumann[ac] and Martin K. Beyer[*bd]

DOI: 10.1039/b000000x [DO NOT ALTER/DELETE THIS TEXT]

AFM-based dynamic single-molecule force spectroscopy was used to stretch carboxymethylated amylose (CMA) polymers, which have been covalently tethered between a silanized glass substrate and a silanized AFM tip via acid-catalyzed ester condensation at pH 2.0. Rupture forces were measured as a function of temperature and force loading rate in the force-ramp mode. The data exhibit significant statistical scattering, which is fitted with a maximum likelihood estimation (MLE) algorithm. Bond rupture is described with a Morse potential based Arrhenius kinetics model. The fit yields a bond dissociation energy D_e = 35 kJ mol^{-1} and an Arrhenius pre-factor A = 6.6×10^4 s^{-1}. The bond dissociation energy is consistent with previous experiments under identical conditions, where the force-clamp mode was employed. However, the bi-exponential decay kinetics, which the force-clamp results unambiguously revealed, is not evident in the force-ramp data. While it is possible to fit the force-ramp data with a bi-exponential model, the fit parameters differ from the force-clamp experiments. Overall, single-molecule force spectroscopy in the force-ramp mode yields data whose information content is more limited than force-clamp data. It may, however, still be necessary and advantageous to perform force-ramp experiments. The number of successful events is often higher in the force-ramp mode, and competing reaction pathways may make force-clamp experiments impossible.

1 Introduction

Covalent mechanochemistry has been rapidly developing over the last decade.[1–3] Quantitative theory has matured, with a variety of approaches available for a wide range of problems, like COnstrained Geometry simulates External Force (COGEF),[4] External Force Explicitly Included (EFEI),[5] Force Modified Potential Energy Surfaces (FMPES)[6] including approximate models based on numerical expansion of the FMPES.[7] For quantitative experiments, the instrument of choice is the atomic force microscope (AFM). Since its introduction in 1994,[8] AFM based single–molecule force spectroscopy (SMFS) has been successfully applied in a versatile manner from the investigation of receptor ligand interactions,[8–10] protein folding,[11–15] adhesion forces and polymer elasticity,[16–23] to studies addressing the mechanical properties of covalent bonds.[1,24–29]

In early SMFS surveys, intermolecular and intramolecular forces were extracted independently of the involved mechanical transient by approximating a constant force-loading rate.[8,24] By expanding this strategy to the dynamic SMFS approach,

where the force-loading rate is varied over an appropriate range, a typically nearly linear relationship between binding strength and the logarithm of the force-loading rate can be found. Thus, the structural and kinetic parameters of the underlying process become accessible.[13,30–32]

In order to obtain the kinetic parameters from such dynamic SMFS experiments, different theoretical models have been developed,[4,33–36] all considering bond rupture as a thermally activated process, where the activation barrier is lowered by the mechanical energy stored in the deflected cantilever. A general description of such a thermally activated rupture process is provided by Arrhenius type kinetics, with a force-dependent activation energy E_a, where the bond lifetime $\tau = 1/k^{off}$ is given by $k^{off} = A \exp[-E_a(f)/k_BT]$.

For the theoretical description of covalent bonds under mechanical load, an Arrhenius kinetics model combined with a Morse potential has been widely used as an approximation.[4,35,37,38] With the force-dependent deformation of the Morse potential, which enters the force-dependent activation energy in the Arrhenius equation, bond rupture probabilities can be numerically calculated and the dynamics, as well as the structural parameters of these single bond rupture events, can be extracted from the experimental data.[26]

A more recent approach in the realm of AFM–based SFMS is the force–clamp SMFS method, where an individually coupled molecule is stretched with a defined force, and retained at this force until bond scission occurs. The recorded force versus time plot yields the bond survival time as a function of clamp force and temperature. A large number of statistically distributed bond survival times provides the complete unimolecular kinetics of the bond dissociation event, and allows for distinguishing multiexponential decay kinetics.[39] In contrast to dynamic SMFS, the force–clamp SMFS technique provides direct access to the reaction kinetics of mechanically activated processes on the molecular level.[12,14,15,40–43] By analyzing the recorded data with an Arrhenius kinetics model with a force-dependent activation barrier, the measured reaction rate constants can be used directly to calculate force and temperature-independent parameters, like the activation energy, the Arrhenius pre-factor and the width of the binding potential.

In a recent study,[39] we took advantage of force–clamp SMFS to record force and temperature-dependent bond survival times of carboxymethylated amylose (CMA) covalently tethered to silane functionalized silicon oxide surfaces via acid-catalyzed ester condensation at pH 2.0.[44] The conducted experiments revealed bi-exponential rupture kinetics, which has been rationalized with the silyl ester hydrolysis depending on the moieties at the silicon atom under acidic conditions.

Here, we have performed temperature-dependent dynamic SMFS to stretch individual CMA polymers under similar conditions in order to determine the structural parameters of the binding potential, i.e. the bond dissociation energy D_e, the parameter β^{-1}, which is proportional to the potentials width, and the Arrhenius pre-factor A. Comparing the obtained data with the results from force–clamp SMFS[39] reaffirm the assumption of a silyl ester hydrolysis mechanism. The advantages and disadvantages of force–clamp SMFS and the more widely used dynamic SMFS method are discussed.

2. Experimental procedure and data analysis

2.1 Materials

Carboxymethylated amylose (CMA), N^1-[3-(trimethoxysilyl)-propyl]diethylene-triamine (DETA), and phosphate buffered saline (PBS; buffer composed of 0.137 M NaCl, 0.010 M Na_2HPO_4, 0.003 M KCl, and 0.002 M KH_2PO_4, pH 7.4 at T = 25 °C), were purchased from Sigma-Aldrich (Deisenhofen, Germany). Hydrochloric acid (32% GR for analysis), acetic acid (99-100% for synthesis), and ethanol (absolute GR for analysis) were obtained from Merck (Darmstadt, Germany). All experiments were performed with silicon nitride AFM cantilevers with a nominal force constant between 10 and 20 mNm^{-1} (MLCT-AU, Veeco Instruments GmbH, Mannheim, Germany). Glass microscope slides were obtained from Menzel (Braunschweig, Germany).

2.2 Experimental Setup

Sample preparation was performed as previously described.[39,44] Glass microscope slides were immersed in diluted hydrochloric acid for 120 min, sonicated in the cleaning solution for 60 min, and rinsed with water three times. Silicon nitride AFM cantilevers were irradiated with UV light for 60 min and immersed in ethanol. Glass slides and cantilever surfaces were functionalized with DETA by immersion for 60 min in a 10:1 ethanol:water mixture, acidified with acetic acid to pH 4.5-5.5, with a DETA content of 2 vol %. After rinsing with ethanol, slides and cantilevers were cured at 110 °C for 20 min. Prior to individual SMFS experiments, CMA was suspended in PBS titrated to pH 2.0 with diluted hydrochloric acid and transferred to the functionalized glass substrate, followed by thorough rinsing. The slide was then mounted on the AFM stage and covered with PBS buffer, which was also acidified to pH 2.0. Previous experiments with DETA and three other organosilanes under identical experimental conditions showed that CMA is linked to DETA via an acid-catalyzed ester condensation.[44]

In order to perform temperature-dependent SMFS experiments, a thermostat (CF30 Kryo-Kompakt-Thermostat, Julabo Labortechnik GmbH, Seelbach, Germany) was connected with a fluid cooler (FLKU 140 G 200, Fischer Elektronik GmbH, Lüdenscheid, Germany) serving as slide holder, as described elsewhere.[26] After a constant temperature of the solution at the stage was obtained, SMFS experiments were conducted using an atomic force microscope (NanoWizard, JPK Instruments, Berlin, Germany) in the force spectroscopy mode. The AFM tip was approached to the glass substrate with covalently coupled CMA, and force vs. distance curves were recorded. The maximum contact force between AFM tip and substrate prior to recording a force vs. distance curve was kept below 0.3 nN, and the contact time between AFM tip and substrate was kept between 0.5 s and 1.0 s.

2.3 Data Analysis

The experimental results were analyzed in a parallel fit procedure using a Morse potential based Arrhenius rate equation as previously described in detail.[26] Force-loading rate-dependent bond rupture distributions were numerically calculated and optimized by varying the parameters D_e, f_{max}, and A. In order to account for the exact shape of the bond rupture distributions, parameter optimization was performed with the maximum likelihood estimator method.[45] For reasons of better comparability with the results obtained from force–clamp SMFS experiments, the Arrhenius pre-

factor A was treated as a temperature-independent parameter and the potential width β^{-1} was calculated via $\beta = 2f_{max}/D_e$.[4] Parameter errors were calculated as previously described[39] with the MINOS algorithm, which is included in the MINUIT analysis tool.[46] The optimum parameters obtained from the MLE procedure were varied until the maximum of the log-likelihood function was reduced by the value 0.5, which defines the confidence interval of 68.3%.[47]

3. Results and Discussion

Scheme 1 displays a single CMA polymer tethered between glass substrate and AFM tip via silyl ester bonds. These bonds are formed under acidic conditions, where a proton catalyzed condensation reaction takes place between carboxyl groups in the CMA and unreacted hydroxyl groups on the glass surface or on the silane surface anchor.[38]

When the cantilever retracts at a constant velocity from the surface, the individually picked up CMA molecule is stretched until the connection between AFM tip and substrate is lost. One can obtain the bond rupture force as well as the force-loading rate from the resulting force-extension curve.[27] Variation of the retract velocity allows to cover a wide range of force-loading rates $\dot{f}$. If the force-loading rate is systematically varied, scatter plots can be obtained as shown in Figure 1, where the bond rupture force is plotted versus the force-loading rate.

In order to extract the kinetic parameters from the measured data recorded at five temperatures between 282 K and 320 K, the five data sets were analyzed with a parallel fit procedure using an Arrhenius kinetics model in combination with a Morse potential, as previously described.[27] In brief, force-loading rate-dependent rupture force probability distributions were optimized for all five temperatures using the maximum likelihood estimation (MLE) method.

The rupture force distributions (green shaded areas) shown in Figure 1 were calculated with the obtained fit parameters D_e = 35 kJ mol^{-1}, β^{-1} = 0.061 Å, and the corresponding Arrhenius pre-factor $A = 6.6\times10^4$ s^{-1}. The extracted parameters are summarized in Table 1 and compared to values as determined from experiments conducted under similar conditions using force–clamp SMFS.

The bond dissociation energy D_e = 34.7 kJ mol^{-1} as well as the Arrhenius pre-factor $A = 6.6\times10^4$ s^{-1} determined from dynamic SMFS are almost identical with the ones obtained for the slow process from force–clamp SMFS experiments, pointing towards the observation of identical bond rupture processes in both, the dynamic and the force–clamp SMFS approach. This serves as a first hint, that the two AFM-based techniques provide consistent kinetic parameters on the single–molecule level, which clearly demonstrates the reliability of the two SMFS strategies. However, the parameters from dynamic SMFS correspond to the parameters for the slow process and slightly differ from the values for the fast process, which become evident under force-clamp conditions. Together with β^{-1} = 0.061 Å, which is found to be twice as large as the values extracted from force–clamp SMFS experiments, the observed variations may be explained by systemic differences concerning data extraction and analysis.

The most obvious difference between the two experimental approaches is given by the fact that experiments conducted by means of dynamic SMFS do not allow for the distinction of multi-exponential kinetics, i.e. different subsets of decays typically remain undetected. This can be attributed to the force-loading rate dependence in the

case of dynamic SMFS: while force–clamp SMFS experiments directly yield reaction rate constant(s) $k(f,T)$, which depend on clamp force and temperature, the reaction rate constant, which determines the data obtained from dynamic SMFS experiments, additionally depends on the force-loading rate, i.e. $k(f,\dot{f},T)$. As a consequence, with force-loading rate as an additional variable, the experimental data from dynamic SMFS investigations can be described by an arbitrary number of reaction rate constants, which makes a clear distinction of multiple decays practically impossible. Consequently, if the values from dynamic SMFS summarized in Table 1 actually result from a bi-exponential decay, one has to work with the assumption that the dynamic SMFS parameters represent the optimum compromise between the parameters extracted from the two processes using force–clamp SMFS. However, fitting a data set, which apparently consists of two superimposed data entities, with one single parameter set, might be expected to be accompanied by higher parameter errors due to the influence of larger data scattering. As can be seen from Table 1, the contrary is the case here.

The fact that the parameter errors are even larger for the values extracted from force–clamp SMFS, can be ascribed to the assumption of an inconsistent bond rupture distribution in order to analyze the data recorded with dynamic SMFS. Generally, the MLE-based parameter optimization aims for a bond rupture distribution that makes the observed data most probable, i.e. the most likely probability for the ensemble of data point is calculated by varying the unknown fit parameters.[45] The latter is crucial in order to obtain consistent parameter estimates for the observed data. By analyzing two sub-processes with one single set of bond rupture distributions, parameters corresponding to the best fit are indeed found, but the underlying model assumption is inconsistent with the observations from force–clamp SMFS.

As a consequence, in order to be able to directly compare the parameters from dynamic SMFS and force–clamp SMFS, modelling the data shown in Figure 1 with two bond rupture distribution sets is inevitable. Figure 2 shows the results of such a fit, where the branching ratio between the two processes has been treated as a fit parameter. As expected, with the higher flexibility of the fit, the likelihood function improves significantly. This alone is not unambiguous proof that the bi-exponential fit is more correct. The fact, however, that the branching ratio between the slow and the fast process is similar to the fit of the force-clamp results indicates that the two data sets are consistent, and that the key idea of a bi-exponential behaviour is correct. The fit parameters for the slow process are $D_{e,s}$ = 54.9 kJ mol^{-1}, β^{-1}_{s} = 0.117 Å, and an Arrhenius pre-factor of $A_s = 2.0\times10^5$ s^{-1}, for the fast process they are $D_{e,f}$ = 36.9 kJ mol^{-1}, β^{-1}_{f} = 0.098 Å, and an Arrhenius pre-factor of $A_f = 2.5\times10^4$ s^{-1}. The two processes contribute with a weight factor of 0.32 for the slow and 0.68 for the fast process. The results of the force-ramp and force clamp fits are summarized in Table 1 to facilitate comparison.

The parameters of the dominant fast process, in particular the dissociation energy D_e, compare favorably with the single-exponential fit. The force-clamp results deviate slightly for the fast process, where a higher dissociation energy is compensated by a higher pre-factor A. Significantly different, however, is the dissociation energy for the slow process. With 54.9 kJ/mol, it is 15.7 kJ/mol higher than the corresponding value from the force-clamp fit, and lies well outside the numerical error limits. This may in part be due to the smaller contribution of the slow process. More likely, however, is a systematic problem. The Morse potential

based Arrhenius kinetics model, initially developed for the homolytic rupture of a covalent bond in the polymer backbone, is not a very good approximation for the potential energy surface of bond hydrolysis. In the absence of a better model, it is still worthwhile to conduct these fits. A fully consistent picture, with quantitatively reliable results, however, will only emerge when a realistic description of the potential energy surface of the reaction is available and implemented into the fit procedure.

4. Conclusions

In the present study, we have identified structural and kinetic parameters for the mechanically induced rupture of individual covalent bonds using temperature-dependent dynamic SMFS at pH 2.0. Except for the slow process of the bi-exponential fit, the kinetic parameters agree well with the ones extracted from force–clamp SMFS experiments performed under acidic conditions. This clearly indicates the observation of the analogous bond rupture mechanism. The results corroborate that silyl ester hydrolysis is observed at low pH. The consistent results first of all demonstrate the functional equivalence of the two AFM-based single–molecule approaches. However, unambiguous identification of a bi-exponential behaviour, which has been clearly evident in force–clamp SMFS, appeared to be impossible with the dynamic SMFS technique. As a consequence, analyzing the data presented here on the basis of one single bond rupture mechanism yields parameters, which are directly comparable to the parameters from force–clamp SMFS with reservations only. When the analysis model is extended to account for two isomeric decays, dynamic SMFS experiments yield results that deviate from the force-clamp experiments. This may in part be attributed to the low number of recorded bond rupture events per force-loading rate representing a statistically weak data basis for the calculation of two weighted bond rupture distributions. Another limitation is the use of a Morse potential to describe the potential energy surface of a hydrolysis reaction.

Experiments conducted in the force–clamp SMFS mode with clamp force as controllable experimental parameter, allow for the direct observation of multiple isomeric decays. This substantial advantage considerably extends the capabilities of AFM-based SMFS methods to the extraction of kinetic parameters from multi-exponential processes on the single–molecule level, which are hardly accessible with the widely used dynamic SMFS approach. Force-ramp experiments will still be useful in cases where the number of successful events is too low in the force-clamp mode, and where the force-distance curve yields additional information.

Acknowledgments

S.W.S., M.F.P. and H.C.-S. gratefully acknowledge financial support of the German Excellence Initiative via the “Nanosystems Initiative Munich (NIM)”. M.K.B. gratefully acknowledges funding from the Sonderforschungsbereich 677 “Function by Switching” supported by the Deutsche Forschungsgemeinschaft (DFG).

References

[a] *Munich University of Applied Sciences, Department of Applied Sciences and Mechatronics, Lothstr. 34, 80335 Munich, Germany. Fax: +49 89 1265 1603; Tel:+49 89 1265 1615; E-mail: clausen-schaumann@hm.edu;alfred.kersch@hm.edu*
[b] *Institut für Physikalische Chemie, Christian-Albrechts-Universität zu Kiel, Olshausenstrasse 40, 24098 Kiel, Germany.*
[c] *Center for NanoScience (CeNS), Geschwister-Scholl-Platz 1, 80539 Munich, Germany.*
[d] *Institut für Ionenphysik und Angewandte Physik, Leopold-Franzens-Universität Innsbruck, Technikerstrasse 25, 6020 Innsbruck, Austria. Fax: +43 512 507 2932; Tel: +43 512 507 52680; E-mail: martin.beyer@uibk.ac.at*

1 M. K. Beyer and H. Clausen-Schaumann, *Chem. Rev.*, 2005, 105, 2921.
2 M. M. Caruso, D. A. Davis, Q. Shen, S. A. Odom, N. R. Sottos, S. R. White and J. S. Moore, *Chem. Rev.*, 2009, 109, 5755.
3 J. Ribas-Arino and D. Marx, *Chem. Rev.*, 2012, 112, 5412.
4 M. K. Beyer, *J. Chem. Phys.*, 2000, 112, 7307.
5 J. Ribas-Arino, M. Shiga and D. Marx, *Angew. Chem. Int. Ed.*, 2009, 48, 4190.
6 M. T. Ong, J. Leiding, H. Tao, A. M. Virshup and T. J. Martínez, *J. Am. Chem. Soc.*, 2009, 131, 6377.
7 A. Bailey and N. J. Mosey, *J. Chem. Phys.*, 2012, 136, 44102.
8 E. L. Florin, V. T. Moy and H. E. Gaub, *Science*, 1994, 264, 415.
9 P. Hinterdorfer, W. Baumgartner, H. J. Gruber, K. Schilcher and H. Schindler, *P. Natl. Acad. Sci. U.S.A.*, 1996, 93, 3477.
10 F. Schwesinger, R. Ros, T. Strunz, D. Anselmetti, H.-J. Guntherodt, A. Honegger, L. Jermutus, L. Tiefenauer and A. Pluckthun, *P. Natl. Acad. Sci. U.S.A.*, 2000, 97, 9972.
11 M. Rief, M. Gautel, F. Oesterhelt, J. M. Fernandez and H. E. Gaub, *Science*, 1997, 276, 1109.
12 A. F. Oberhauser, P. K. Hansma, M. Carrion-Vazquez and J. M. Fernandez, *P. Natl. Acad. Sci. U.S.A.*, 2001, 98, 468.
13 M. Rief and H. Grubmüller, *ChemPhysChem*, 2002, 3, 255.
14 J. M. Fernandez and H. B. Li, *Science*, 2004, 303, 1674.
15 B. Bullard, T. Garcia, V. Benes, M. C. Leake, W. A. Linke and A. F. Oberhauser, *P. Natl. Acad. Sci. U.S.A.*, 2006, 103, 4451.
16 M. Rief, F. Oesterhelt, B. Heymann and H. E. Gaub, *Science*, 1997, 275, 1295.
17 P. E. Marszalek, A. F. Oberhauser, Y. P. Pang and J. M. Fernandez, *Nature*, 1998, 396, 661.
18 T. Hugel, M. Grosholz, H. Clausen-Schaumann, A. Pfau, H. Gaub and M. Seitz, *Macromolecules*, 2001, 34, 1039.
19 Z. Lu, W. Nowak, G. Lee, P. E. Marszalek and W. Yang, *J. Am. Chem. Soc.*, 2004, 126, 9033.
20 E. Thormann, D. R. Evans and V. S. J. Craig, *Macromolecules*, 2006, 39, 6180.
21 Q. Zhang and P. E. Marszalek, *Polymer*, 2006, 47, 2526.
22 M. I. Giannotti and G. J. Vancso, *ChemPhysChem*, 2007, 8, 2290.
23 K. Liu, Y. Song, W. Feng, N. Liu, W. Zhang and X. Zhang, *J. Am. Chem. Soc.*, 2011, 133, 3226.
24 M. Grandbois, M. Beyer, M. Rief, H. Clausen-Schaumann and H. E. Gaub, *Science*, 1999, 283, 1727.
25 P. Schwaderer, E. Funk, F. Achenbach, J. Weis, C. Bräuchle and J. Michaelis, *Langmuir*, 2008, 24, 1343.
26 S. W. Schmidt, A. Kersch, M. K. Beyer and H. Clausen-Schaumann, *Phys. Chem. Chem. Phys.*, 2011, 13, 5994.
27 S. W. Schmidt, M. K. Beyer and H. Clausen-Schaumann, *J. Am. Chem. Soc.*, 2008, 130, 3664.
28 J. Liang and J. M. Fernández, *J. Am. Chem. Soc.*, 2011, 133, 3528.
29 H. M. Klukovich, T. B. Kouznetsova, Z. S. Kean, J. M. Lenhardt and S. L. Craig, *Nature Chem.*, 2012, 5, 110.
30 R. Merkel, P. Nassoy, A. Leung, K. Ritchie and E. Evans, *Nature*, 1999, 397, 50.
31 B. Heymann and H. Grubmüller, *Phys. Rev. Lett.*, 2000, 84, 6126.
32 T. Hugel and M. Seitz, *Macromol. Rapid Comm.*, 2001, 22, 989.
33 G. I. Bell, *Science*, 1978, 200, 618.
34 E. Evans and K. Ritchie, *Biophys. J.*, 1997, 72, 1541.
35 F. Hanke and H. J. Kreuzer, *Phys. Rev. E*, 2006, 74, 31909.
36 O. Dudko, G. Hummer and A. Szabo, *Phys. Rev. Lett.*, 2006, 96, 108101.

37 W. Kauzmann and H. Eyring, *J. Am. Chem. Soc.*, 1940, 62, 3113.
38 M. F. Iozzi, T. Helgaker and E. Uggerud, *Mol. Phys.*, 2009, 107, 2537.
39 S. W. Schmidt, P. Filippov, A. Kersch, M. K. Beyer and H. Clausen-Schaumann, *ACS Nano*, 2012, 6, 1314.
40 A. P. Wiita, S. R. K. Ainavarapu, H. H. Huang and J. M. Fernandez, *P. Natl. Acad. Sci. U.S.A.*, 2006, 103, 7222.
41 S. R. K. Ainavarapu, A. P. Wiita, L. Dougan, E. Uggerud and J. M. Fernandez, *J. Am. Chem. Soc.*, 2008, 130, 6479.
42 R. Szoszkiewicz, S. R. K. Ainavarapu, A. P. Wiita, R. Perez-Jimenez, J. M. Sanchez-Ruiz and J. M. Fernandez, *Langmuir*, 2008, 24, 1356.
43 J. Liang and J. M. Fernández, *ACS Nano*, 2009, 3, 1628.
44 S. W. Schmidt, T. Christ, C. Glockner, M. K. Beyer and H. Clausen-Schaumann, *Langmuir*, 2010, 26, 15333.
45 S. Brandt, *Data analysis. Statistical and computational methods for scientists and engineers*, Springer, New York, 3rd edn., 1999.
46 F. James and M. Roos, *Comp. Phys. Comm.*, 1975, 10, 343.
47 CN/ASD Group, *MINUIT - Users Guide. nProgram Library D506*, CERN, 1993.

Tables

Table 1 Parameters extracted from experimental data using an Arrhenius kinetics model in combination with a Morse potential

Parameter[a]	Dynamic SMFS[bd]	Dynamic SMFS[cd]		Force-Clamp SMFS[ef]	
		slow	fast	slow	fast
D_e / kJ mol^{-1}	34.7±1.2	54.9±2.3	36.9±1.7	39.2±5.7	39.5±5.1
β^{-1} / Å	0.061±0.023	0.117±0.005	0.098±0.011	0.033±0.0035	0.033±0.020
A / s^{-1}	6.6±0.2×10^4	2.0±1.0×10^5	2.5±1.1×10^4	6.0±1.9×10^4	2.0±0.5×10^6

[a]Free parameters from the Morse potential-based Arrhenius kinetics model. [b]Values extracted from the global fit to the experimental data shown in Fig. 1a–e. [c]Experimental data shown in Fig. 2 a-e with a bi-exponential global fit where the slow process is contributing 32% and the fast one 68%. [d]Errors were obtained by calculating the standard-deviation from a numerically calculated hessian matrix. [e]Results from force–clamp SMFS experiments under similar conditions,[39] where a bi-exponential behaviour was found. According to the bi-exponential fit the overall process is subdivided into two fractions, where the slow process contributes 28% and the fast one 72%. [f]Parameters were calculated with the MLE procedure as previously described.[26] The parameter errors correspond to one-standard-deviation errors as calculated according to the MINOS algorithm as part of the MINUIT analysis tool.[47]

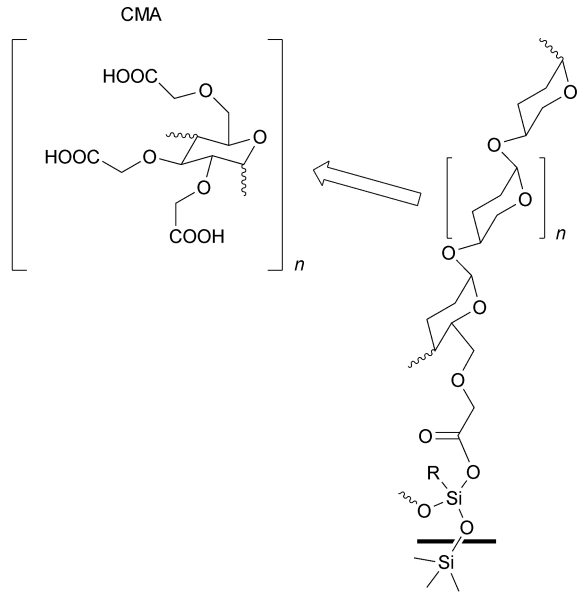

Scheme 1 Individual CMA polymer coupled between silanized AFM tip and silanized substrate. Under acidic conditions, carboxyl groups of the CMA and free hydroxyl groups, which are present either on the substrate surface (top) or on free silanol groups in the silane anchor (bottom), undergo proton-catalyzed ester condensation.

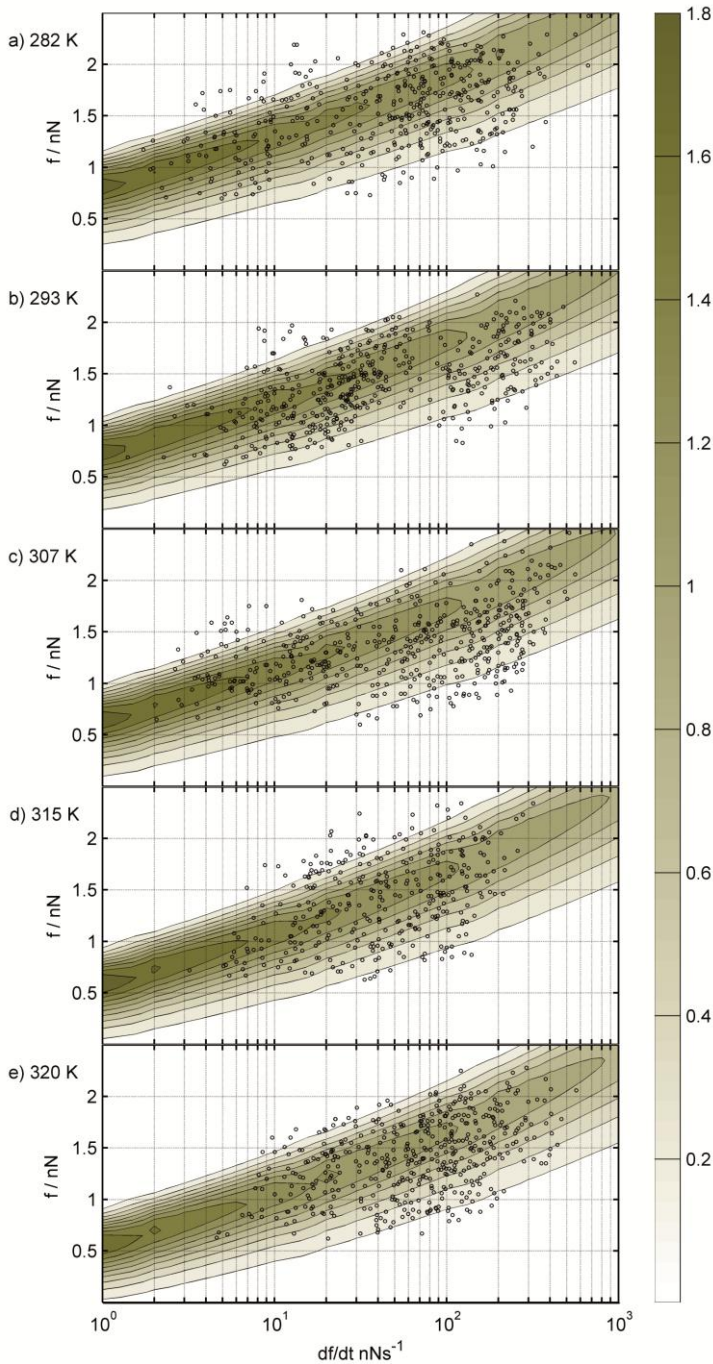

Fig. 1 Bond rupture forces *f* vs. force loading rates d*f*/d*t* of more than 2150 single molecule rupture events at 282 K (a), 293 K (b), 307 K (c), 315 K (d), and 320 K (e). Every data point corresponds to one individual rupture event. The green shaded areas show the expected distribution calculated with the fit parameters D_e = 34.7 kJ mol^{-1}, β^{-1} = 0.061 Å, and an Arrhenius pre-factor of $A = 6.6\times10^4$ s^{-1}.

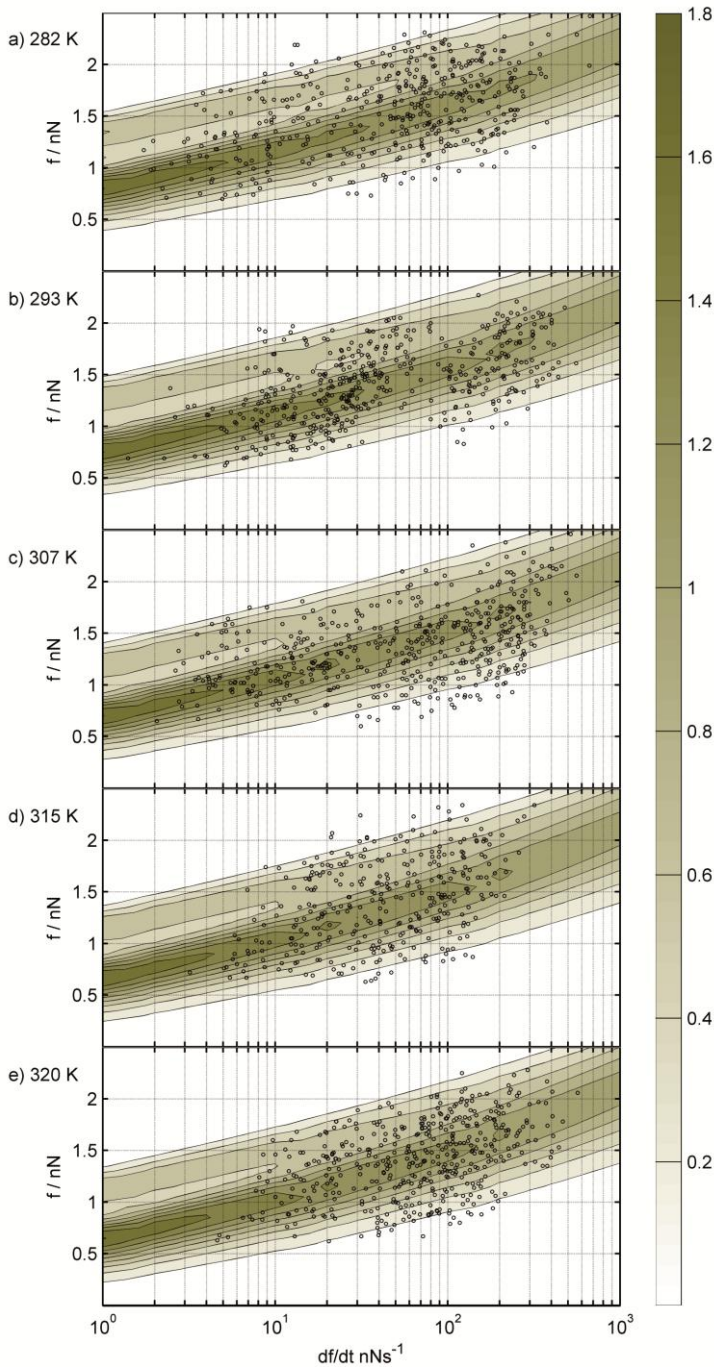

Fig. 2 Here the green shaded areas show the expected distribution calculated with the bi-exponential fit parameters for the slow process of $D_{e,s}$ = 54.9 kJ mol^{-1}, $\beta^{-1}{}_s$ = 0.117 Å, and an Arrhenius pre-factor of $A_s = 2.0\times10^5$ s^{-1}, for the fast process of $D_{e,f}$ = 36.9 kJ mol^{-1}, $\beta^{-1}{}_f$ = 0.098 Å, and an Arrhenius pre-factor of $A_f = 2.5\times10^4$ s^{-1}. The two processes are combined with a weight factor of 0.32 for the slow and 0.68 for the fast process.

Table of Contents Entry

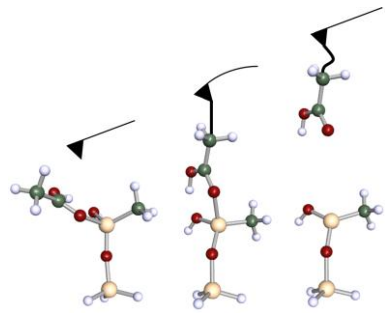

Carboxymethylated amylose is anchored via silyl ester bonds between an AFM cantilever tip and a glass substrate at pH 2.0. Rupture forces of the bonds are measured in the force-ramp mode, and strategies for statistical data analysis are discussed.